

Multiple scattering and energy loss in semi-inclusive deeply inelastic eA scattering

Xiaofeng Guo^{*} and Jun Li[†]

*Department of Physics and Astronomy,
Iowa State University, Ames, IA 50011*

(Dated: February 8, 2022)

Abstract

We calculate the multiple scattering effect on single hadron production in semi-inclusive lepton-nucleus deeply inelastic scattering. We show that the quantum interference of multiple scattering amplitudes leads to suppression in hadron productions. At the leading power in medium length, the suppression can be approximately expressed in terms of a shift in z of the fragmentation function $D(z)$, and could be therefore interpreted as the collisional energy loss. We compare our calculation with existing experimental data. We also discuss the effect of quark mass on the suppression. Our approach can be extended to other observables in hadronic collisions.

^{*}Electronic address: gxf@iastate.edu

[†]Electronic address: junli@iastate.edu

I. INTRODUCTION

The understanding of parton propagation through the nuclear environment is crucial for the interpretation of physics phenomena observed at the Relativistic Heavy Ion Collider(RHIC) and future Large hadron Collider(LHC). The observed strong suppression of high transverse momentum hadron at RHIC was considered to be an evidence for the QCD quark-gluon plasma [1]. The suppression was believed to be the result of medium induced radiative energy loss of high energy partons [2]. However, recent data indicate that heavy quarks would have to lose the same amount of energy as that of a light quark if the radiative energy loss is the only source of the suppression [3]. On the other hand, we expect heavy quarks to lose much less energy than a light quark because of its mass [4]. This discrepancy attracted significant theoretical interests in searching for other causes of parton energy loss [5]. Several studies suggested that the collisional energy loss could be an important source of the observed discrepancy [6]. Because of QCD confinement, we can not observe partons directly in experiments, instead, we can only observe final state hadrons. The production rate could be affected by the interference of two scattering amplitudes with the same initial and final hadronic states but with different partonic interactions. In this paper, we study the effect of such quantum interference between two amplitudes with the same as well as different multiple parton-level scattering, and show that the interference leads to a suppression in single hadron production rate, which might be interpreted as the collisional energy loss [5].

The hadronization of partons is a non-perturbative process. However, when the energy scale of the scattering Q is much larger than a typical hadronic scale $1/\text{fm} \sim \Lambda_{QCD}^2$, it is the QCD factorization that allows us to separate the calculable short-distance partonic dynamics from the non-perturbative long-distance physics. The effect of the non-perturbative hadronization process for a parton of flavor f fragmenting to a hadron h is expressed in terms of an universal fragmentation function $D_{f \rightarrow h}(z, \mu_F)$, where z is momentum fraction of the parton carried by the hadron and μ_F is the fragmentation scale. QCD perturbation theory predicts the evolution and the scale dependence on μ_F of the fragmentation function.

Unlike in the vacuum, the fragmenting parton in nuclear medium can have rescattering before the formation of final-state hadrons. The effect of the interaction between the nuclear medium and the propagating parton will manifest itself as changes in parton fragmentation functions. The rescattering can induce extra radiations, and consequently alter the evolution of the fragmentation functions [7, 8], and results in effective parton energy loss [9].

However, quantum mechanically, the parton rescattering in a nuclear medium does not have to induce radiation. Such rescattering can also alter the production rate of the fragmenting parton if it is quantum coherent with the first scattering. Although coherent rescattering is formally suppressed by additional powers of the hard scale, it could be important if the life time of the fragmenting parton is long enough. We show in this paper that quantum interference of two scattering amplitudes with different parton-level rescattering reduces the production rate of the fragmenting parton, which leads to the suppression of hadron productions. In the following sections, we show that such suppression could be effectively expressed as a shift in z for the parton fragmentation functions. This result is complementary to the radiative parton energy loss induced by the rescattering of the fragmenting parton in the nuclear medium.

In general, the production of hadrons can come from both quarks and gluons in hadronic production. However, in the semi-inclusive deep-inelastic lepton-nucleus scattering (SIDIS),

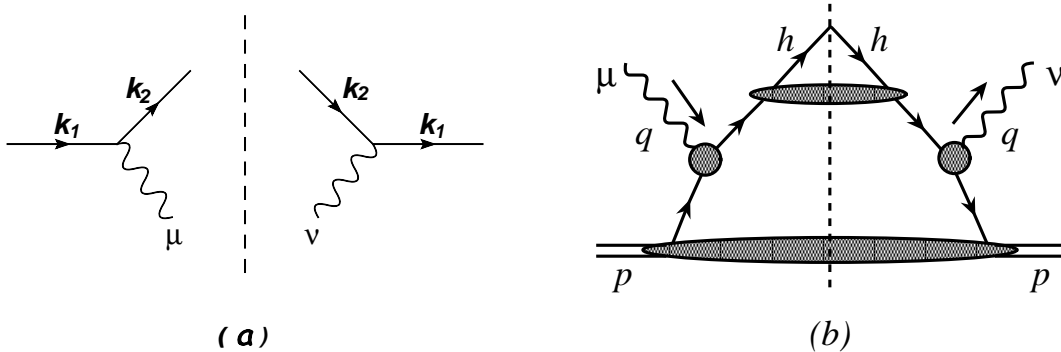


FIG. 1: Factorization for semi-inclusive DIS cross section: (a): the leptonic tensor $L^{\mu\nu}$; (b): the semi-inclusive hadronic tensor.

the leading hadron production is dominated by quarks. It is the ideal place to study the quark energy loss and the knowledge obtained will help us learn more about the gluon energy loss in hadronic productions.

Our paper is organized as follows. In the next section, we first present our derivation of double scattering effect. Then in Sec. III, we show how to generalize it to the n th-scattering and sum up all possible numbers of scatterings, and present the result after the summation. In Sec. IV, we extend our results for light quarks to quarks with finite mass and discuss the effect of quark mass. In Sec. V, we compare our results with experimental data from HERMES. We also discuss the applicable ranges of z value for our result and propose a model for larger z region. Finally, in Sec. VI, we summarize our work and discuss extensions of our approach to other observables in hadronic collisions.

II. DOUBLE SCATTERING CONTRIBUTION

We consider the semi-inclusive DIS production of a single hadron of momentum p_h ,

$$e(k_1) + A(p) \longrightarrow e(k_2) + h(p_h) + X, \quad (1)$$

where k_1 and k_2 are the four momenta of the incoming and the outgoing leptons respectively, p is the average momentum per nucleon for the nucleus with the atomic number A . To study the nuclear effects, we compute the hadron production rate per DIS event,

$$R^A = \frac{d\sigma_{eA \rightarrow ehX}}{dx_B dQ^2 dz} \bigg/ \frac{d\sigma_{eA \rightarrow eX}}{dx_B dQ^2}; \quad (2)$$

where $d\sigma_{eA \rightarrow eX}/dx_B dQ^2$ is the inclusive DIS cross section. In Eq. (2), the Bjorken variable $x_B = Q^2/(2p \cdot q)$ with the virtual photon momentum $q^\mu = (k_1 - k_2)^\mu$ and $Q^2 = -q^2$. We work in photon-nucleus frame, and choose the target momentum p along \hat{z} -axis, such that $p^\mu = (p^0, p^x, p^y, p^z) = (P, 0, 0, P)$, and only $p^+ = (p^0 - p^z)/\sqrt{2}$ is nonvanishing, neglecting target mass. In this frame, the nucleus is moving in the “+” direction. The struck quark propagates along the “−” direction and could interact coherently with the “remnants” of the nucleus. The hadron momentum fraction z_h is defined as

$$z_h \equiv \frac{p \cdot p_h}{p \cdot q} = \frac{2x_B p \cdot p_h}{Q^2}. \quad (3)$$

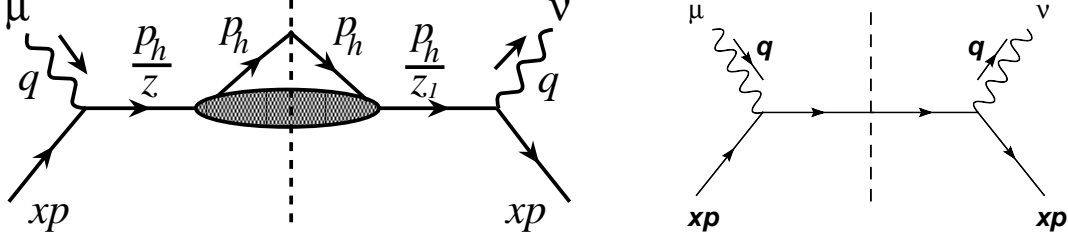


FIG. 2: Lowest order single scattering Feynman diagram for the semi-inclusive hadronic tensor with (a) and without (b) the nonperturbative parton-to-hadron fragmentation attached.

With the approximation of one-photon exchange, the semi-inclusive DIS cross section

$$\frac{d\sigma_{eA \rightarrow ehX}}{dx_B dQ^2 dz_h} = \frac{1}{8\pi} \frac{e^4}{x_B^2 s^2 Q^2} L^{\mu\nu}(k_1, k_2) \frac{dW_{\mu\nu}}{dz_h}, \quad (4)$$

where $s = (p + k_1)^2$ is the total invariant mass of the lepton-nucleon system. In Eq. (4), the leptonic tensor $L^{\mu\nu}$ is given by the diagram in Fig. 1a,

$$L^{\mu\nu}(k_1, k_2) = \frac{1}{2} \text{Tr}(\gamma \cdot k_1 \gamma^\mu \gamma \cdot k_2 \gamma^\nu). \quad (5)$$

The semi-inclusive hadronic tensor $W_{\mu\nu}$ for single scattering contribution is represented in Fig. 1b and can be factorized as

$$\begin{aligned} \frac{dW_{\mu\nu}}{dz_h} &= \sum_q \int dz dz_1 \mathcal{D}_{q \rightarrow h}(z, z_1, Q^2) \int \frac{dx}{x} \delta\left(z - \frac{2xp \cdot p_h}{Q^2}\right) \delta\left(z_1 - \frac{2xp \cdot p_h}{Q^2}\right) \\ &\times \phi_q(x, Q^2) H_{\mu\nu}^{(S)}(x, z, z_1), \end{aligned} \quad (6)$$

where \sum_q runs over (anti)quark flavors, ϕ_q is the leading twist nuclear quark distribution, and $H_{\mu\nu}^{(S)}$ is the partonic part. In Eq. (6) we introduced a two-momentum quark-to-hadron fragmentation density $\mathcal{D}_{q \rightarrow h}(z, z_1, Q^2)$, which is defined as $\int dz_1 \delta(z - z_1) \mathcal{D}_{q \rightarrow h}(z, z_1, Q^2) = D_{q \rightarrow h}(z, Q^2)$ with $D_{q \rightarrow h}$ the normal quark-to-hadron fragmentation function. The z_h -dependence in Eq. (6) is implicit in the argument of the δ -function, $2xp \cdot p_h / Q^2 = (x/x_B)z_h$. In Fig. 2 we show the lowest order Feynman diagram for the semi-inclusive hadronic tensor on a quark state with (a) and without (b) the nonperturbative parton-to-hadron fragmentation attached. Fig. 2b gives the lowest order $H_{\mu\nu}^{(S)}$ [11]:

$$H_{\mu\nu}^{(S)} = \frac{1}{2} e_{\mu\nu}^T \sum_q x e_q^2 \delta\left(x - \frac{Q^2}{2p \cdot q}\right) \quad (7)$$

where e_q is the quark fractional charge, and $e_{\mu\nu}^T$ is defined as

$$e_{\mu\nu}^T = \frac{1}{p \cdot q} [p_\mu q_\nu + q_\mu p_\nu] + \frac{2x_B}{p \cdot q} p_\mu p_\nu - g_{\mu\nu}. \quad (8)$$

Thus, at the lowest order,

$$\frac{dW_{\mu\nu}^{(0)}}{dz_h} = \frac{1}{2} e_{\mu\nu}^T \sum_q \phi_q(x_B, Q^2) D_q(z_h, Q^2), \quad (9)$$

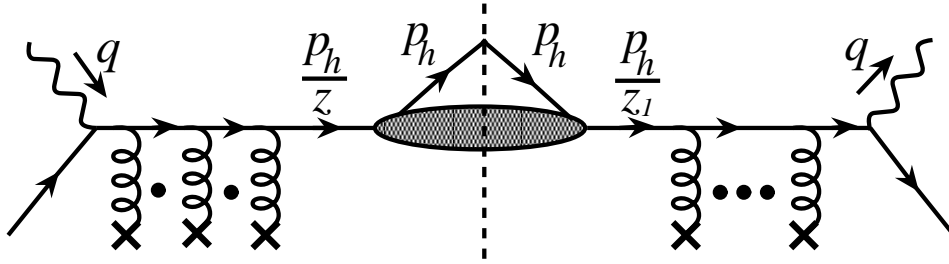


FIG. 3: Sample diagram shows the interference between two amplitudes with the same initial and final states but different partonic scattering.

with z_h defined in Eq. (3).

Single scattering is localized and its medium size dependence is limited to that in the nuclear parton distribution function. We are interested in additional nuclear effects from multiple scattering of the scattered quark and the interference of amplitudes with different partonic scatterings, as sketched in Fig. 3. In this section, we first consider the double scattering contribution to the semi-inclusive hadronic tensor.

Fig. 4 shows leading order double scattering Feynman diagrams for the semi-inclusive hadronic tensor on a quark state. The fermion lines with a short bar represent the contact terms of quark propagators, and diagrams with both gluons attached to the incoming quark line vanish [12]. Although all diagrams in Fig. 4 could contribute to the production rate of the hadron in SIDIS, as we discuss below, only diagrams in Figs. 4(a) and (b) can give the leading power contribution in the $A^{1/3}$ -type medium size enhancement [13]. In terms of Feynman diagram, contribution of every propagator consists of two parts: a potential pole contribution and a contact contribution [12]. For example, a quark propagator of momentum k can always be written as

$$\frac{i\gamma \cdot k}{k^2 + i\epsilon} = \frac{i\gamma \cdot \hat{k}}{k^2 + i\epsilon} + \frac{i\gamma \cdot n}{2k \cdot n} \frac{k^2}{k^2 + i\epsilon}, \quad (10)$$

where $\hat{k}^2 = 0$ and n^μ is any auxiliary vector with $k \cdot n \neq 0$. The first term in the right-hand-side of Eq. (10) corresponds the potential pole contribution when $k^2 \rightarrow 0$, while the second term is the contact contribution [12]. Attaching one gluon to the initial quark line introduces a quark propagator, and this propagator will have both the pole and contact contributions. The pole contribution is long-distance in nature, representing the interactions between the quark and the gluon long before the hard collision between the quark and the virtual photon. The pole contribution of the incoming quark propagator should be part of the nuclear quark distribution, and is partially responsible for the relatively weak A -dependence of the leading-twist parton distributions in a nucleus [14, 15]. On the other hand, the contribution of the contact term is localized in space [12], and does not result into the $A^{1/3}$ type of nuclear enhancement [16]. Since Feynman diagrams in Fig. 4(c) form a gauge invariant subset of short-distance partonic contributions, this set of diagrams will not contribute to the leading $A^{1/3}$ -type of nuclear enhancement. Diagrams with the initial-state contact interactions in Figs. 4(a) and (b) vanish, while the other two diagrams with final-state rescattering will have at least one pole contribution.

The pole contribution from diagrams with the final-state rescattering, shown in Figs. 4(a) and (b), is responsible for the leading $A^{1/3}$ -type of nuclear enhancement, because taking the

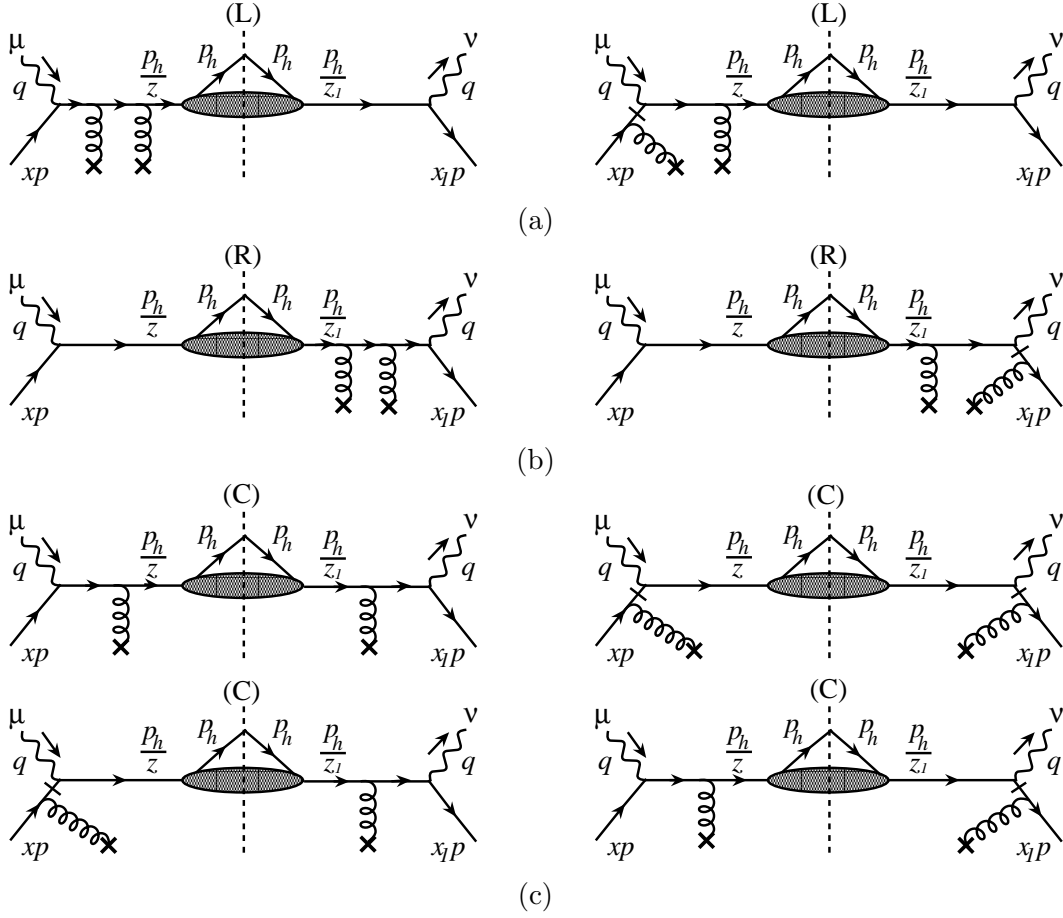


FIG. 4: Leading order double scattering Feynman diagrams that contribute to the semi-inclusive deep inelastic scattering on a quark state. Diagrams of (a) and (b) give explicit $A^{1/3}$ -type medium size enhancement; and diagrams of (c) give localized contributions.

residue of the unpinched pole effectively sets the gluon momentum to zero and leaves the corresponding coordinate space integration of the gluon field to the size of nucleus [13]. Similar to Eq. (6), the factorized form of the leading pole contribution from the double scattering diagrams in Figs. 4(a) and (b) can be expressed as

$$\frac{dW_{\mu\nu}}{dz_h} = \sum_q \int dz dz_1 \mathcal{D}_{q \rightarrow h}(z, z_1, Q^2) \int dx d\tilde{x}_1 dx_1 \delta(z - \frac{2xp \cdot p_h}{Q^2}) \delta(z_1 - \frac{2x_1p \cdot p_h}{Q^2}) \times M_A(x, \tilde{x}_1, x_1) H_{\mu\nu}^{(D)}(x, \tilde{x}_1, x_1, x_B, z, z_1). \quad (11)$$

In Eq. (11), the hadronic matrix element M_A is given by [13]

$$M_A(x, \tilde{x}_1, x_1) = \frac{-1}{x_1 - \tilde{x}_1 - i\epsilon} \frac{1}{\tilde{x}_1 - x - i\epsilon} \int \frac{dy^-}{2\pi} \frac{dy_1^-}{2\pi} \frac{d\tilde{y}_1^-}{2\pi} e^{ixp^+y^-} e^{i(\tilde{x}_1-x)p^+\tilde{y}_1^-} e^{-i(\tilde{x}_1-x_1)p^+y_1^-} \times \langle P_A | \bar{\psi}(0) \frac{\gamma^+}{2} F^{+\alpha}(y_1^-) F_\alpha^+(\tilde{y}_1^-) \psi(y^-) | P_A \rangle. \quad (12)$$

Here we used $F^{+\alpha}(y^-) = n^\rho \partial_\rho A^\alpha(y^-)$ in light-cone gauge. We adapt the $i\epsilon$ prescription introduced in Ref. [18] for the two poles $1/(x_1 - \tilde{x}_1)$ and $1/(\tilde{x}_1 - x)$. If the partonic part,

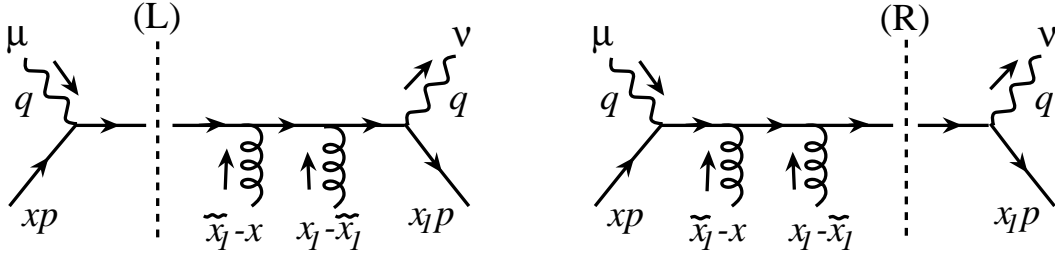


FIG. 5: Lowest order double scattering Feynman diagrams that contribute to the hard part of the leading power $A^{1/3}$ -type nuclear enhancement.

$H_{\mu\nu}^{(D)}(x, \tilde{x}_1, x_1, x_B, z, z_1)$, is a nonvanishing smooth function at the poles, which will be verified later, the two unpinched poles in Eq. (12) can be used to perform the contour integration for $d\tilde{x}_1 dx_1$ in Eq. (11). In this sense, the hadronic matrix element M_A can be effectively written as

$$M_A(x, \tilde{x}_1, x_1) \rightarrow \delta(\tilde{x}_1 - x) \delta(x_1 - \tilde{x}_1) \mathcal{F}_A(x, \tilde{x}_1, x_1) \quad (13)$$

with the function \mathcal{F}_A defined as

$$\begin{aligned} \mathcal{F}_A(x, \tilde{x}_1, x_1) = & \int \frac{dy^-}{2\pi} \frac{dy_1^-}{2\pi} \frac{d\tilde{y}_1^-}{2\pi} e^{ixp^+y^-} e^{i(\tilde{x}_1-x)p^+\tilde{y}_1^-} e^{-i(\tilde{x}_1-x_1)p^+y_1^-} \\ & \times (2\pi)^2 \theta(y_1^-) \theta(\tilde{y}_1^-) \langle P_A | \bar{\psi}(0) \frac{\gamma^+}{2} F^{+\alpha}(y_1^-) F_\alpha^+(\tilde{y}_1^-) \psi(y^-) | P_A \rangle. \end{aligned} \quad (14)$$

The partonic part $H_{\mu\nu}^{(D)}$ in Eq. (11) is given by the Feynman diagrams in Fig. 5 with the quark lines contracted by $\frac{1}{2}\gamma \cdot p$ and gluon lines contracted by $\frac{1}{2}d_{\alpha\beta}$. The transverse tensor $d_{\alpha\beta} = -g_{\alpha\beta} + \bar{n}_\alpha n_\beta + n_\alpha \bar{n}_\beta$ with two lightlike vectors, $n = (n^+, n^-, n_T) = (0, 1, 0_\perp)$ and $\bar{n} = (1, 0, 0_\perp)$. The leading pole contribution of $H_{\mu\nu}^{(D)}$ with cut on the left side is

$$H_{\mu\nu}^{(D)}|_{L-cut} = e_{\mu\nu}^T \left(\frac{1}{2} e_q^2 \right) \left(\frac{2\pi\alpha_s}{3} \right) \frac{1}{Q^2} x_B \frac{\delta(x - x_B)}{x_1 - x}, \quad (15)$$

and the contribution with cut on the right side is

$$H_{\mu\nu}^{(D)}|_{R-cut} = e_{\mu\nu}^T \left(\frac{1}{2} e_q^2 \right) \left(\frac{2\pi\alpha_s}{3} \right) \frac{1}{Q^2} x_B \frac{\delta(x_1 - x_B)}{x - x_1}, \quad (16)$$

with the quark fractional charge e_q and $e_{\mu\nu}^T$ given in Eq. (8). As we can see, the individual contribution of Eqs. (15) and (16) is divergent. However, the sum of the contributions is finite.

Summing up contributions from the both cuts, and using Eqs. (11), (13), (15), and (16),

we have the leading order contribution from the double final state scattering:

$$\begin{aligned} \frac{dW_{\mu\nu}^{(1)}}{dz_h} &\propto \int dz dz_1 \mathcal{D}_{q \rightarrow h}(z, z_1, Q^2) \int dx dx_1 \delta(z - x \frac{2p \cdot p_h}{Q^2}) \delta(z_1 - x_1 \frac{2p \cdot p_h}{Q^2}) \\ &\quad \times \delta(x_1 - x) \mathcal{F}_A(x, x, x_1) \frac{x_B}{Q^2} \left[\frac{\delta(x - x_B)}{x_1 - x} + \frac{\delta(x_1 - x_B)}{x - x_1} \right] \end{aligned} \quad (17)$$

$$\begin{aligned} &= \int dx dx_1 \mathcal{F}_A(x, x, x_1) \int dz dz_1 \delta(x - z \frac{Q^2}{2p \cdot p_h}) \delta(x_1 - z_1 \frac{Q^2}{2p \cdot p_h}) \\ &\quad \times \delta(z - z_1) \mathcal{D}_{q \rightarrow h}(z, z_1, Q^2) \frac{x_B}{Q^2} \frac{Q^2}{2p \cdot p_h} \left[\frac{\delta(z - z_h)}{z_1 - z} + \frac{\delta(z_1 - z_h)}{z - z_1} \right] \end{aligned} \quad (18)$$

with an overall constant factor $(e_{\mu\nu}^T/2) e_q^2 (2\pi\alpha_s/3)$ from the hard parts in Eqs. (15) and (16) and a sum over all quark and antiquark flavor. Because of the $\delta(z - z_1)$, we can expand the z_1 in above expression inside the square bracket around z :

$$\frac{\delta(z - z_h)}{z_1 - z} + \frac{\delta(z_1 - z_h)}{z - z_1} \approx -\delta'(z - z_h) . \quad (19)$$

Combining Eqs. (18) and (19), and carrying out all integrations by using the δ -functions, we have

$$\begin{aligned} \frac{dW_{\mu\nu}^{(1)}}{dz_h} &= \frac{1}{2} e_{\mu\nu}^T \sum_q e_q^2 \left(\frac{4\pi^2\alpha_s}{3} \right) \frac{x_B}{Q^2} \frac{d}{dx_B} T_{qg}^A(x_B, Q^2) D_{q \rightarrow h}(z_h, Q^2) \\ &\quad + \frac{1}{2} e_{\mu\nu}^T \sum_q e_q^2 \left(\frac{4\pi^2\alpha_s}{3} \right) \frac{z_h}{Q^2} T_{qg}^A(x_B, Q^2) \frac{dD_{q \rightarrow h}(z_h, Q^2)}{dz_h} \end{aligned} \quad (20)$$

where \sum_q runs over all quark and antiquark flavors, and the twist-4 quark-gluon correlation function is defined as [17]

$$\begin{aligned} T_{qg}^A(x_B, Q^2) &= \int \frac{dy^-}{2\pi} e^{ix_B p^+ y^-} \int \frac{dy_1^- d\tilde{y}_1^-}{2\pi} \theta(y_1^-) \theta(\tilde{y}_1^-) \\ &\quad \times \langle P_A | \bar{\psi}_q(0) \frac{\gamma^+}{2} F^{+\alpha}(y_1^-) F_{\alpha}^+(\tilde{y}_1^-) \psi_q(y^-) | P_A \rangle . \end{aligned} \quad (21)$$

This result shows that interference of amplitudes with different parton-level multiple scatterings affects the hadron production rate in SIDIS. The effect is sensitive to the slope of incoming parton flux as well as the shape of the fragmentation function. When combined with the lowest order in Eq. (9), the first term in Eq. (20) is responsible for the high twist shadowing of inclusive deep inelastic scattering (DIS) [10]. The same effect should also appear in the denominator of Eq. (2), and therefore, it will not be included in the rest of the discussion for the hadron production rate defined in Eq. (2).

From Eq. (17), we can also derive Eq. (20) by first expanding x_1 around x utilizing the δ -function $\delta(x_1 - x)$:

$$\frac{\delta(x - x_B)}{x_1 - x} + \frac{\delta(x_1 - x_B)}{x - x_1} \approx -\delta'(x - x_B) , \quad (22)$$

and then integrating over $dx dx_1$ and $dz dz_1$. In next section, when we calculate the higher order multiple scattering effect, we will follow this derivation to make the presentation simpler.

III. GENERALIZE TO HIGHER ORDER MULTIPLE SCATTERING

To compute the effect of higher order final state multiple scattering, we add pairs of gluon interactions to the struck quark and convert the gluon field operators in the hadronic matrix element of $W^{\mu\nu}$ to the corresponding field strength. Each pair of gluon interaction will contribute a factor of [10]

$$x_B \frac{2\pi\alpha_s}{3Q^2} \int \frac{dy_i^-}{2\pi} \frac{d\tilde{y}_i^-}{2\pi} \frac{e^{i(x_i-\tilde{x}_i)p^+y_i^-}}{x_i-\tilde{x}_i-i\epsilon} \frac{e^{i(\tilde{x}_i-x_{i-1})p^+\tilde{y}_i^-}}{\tilde{x}_i-x_{i-1}-i\epsilon} F^{+\alpha}(y_i^-) F_\alpha^+(\tilde{y}_i^-) \left\{ \begin{array}{ll} \frac{-1}{x_{i-1}-x_B+i\epsilon} & \text{(L)} \\ \frac{-1}{x_i-x_B-i\epsilon} & \text{(R)} \end{array} \right. \cdot \quad (23)$$

“L” (“R”) means the gluon pair are to the left (right) of the final state cut line.

To obtain the leading pole contribution for the partonic part with n additional scattering, we need to sum over all diagrams with all possible insertions of the n gluon pairs to both sides of the final state cut line. Similar to Eq. (13) we can replace the poles in Eq. (23) by corresponding δ - functions, expand all x_i of $\delta(x_i - x)$ around x , and obtain

$$H_{\mu\nu}^{(n)} = e_{\mu\nu}^T \left(\frac{1}{2} e_q^2 \right) \left(\frac{2\pi\alpha_s}{3} \right)^n \left(\frac{x_B}{Q^2} \right)^n (-1)^n \frac{d^n}{dx} \delta(x - x_B). \quad (24)$$

Convoluting $H_{\mu\nu}^{(n)}$ with the fragmentation function and following similar derivations for the double scattering case, we obtain the leading pole contribution for semi-inclusive hadronic tensor, with n additional scattering:

$$\frac{dW_{\mu\nu}^{(n)}}{dz_h} \approx \frac{1}{2} e_{\mu\nu}^T \sum_q e_q^2 \left[z_h \frac{4\pi^2\alpha_s}{3Q^2} \right]^n \frac{1}{n!} M_A^{(n)}(x_B, Q^2) \frac{d^n}{dz_h^n} D_{q \rightarrow h}(z_h, Q^2) \quad (25)$$

with the multi-field matrix element M_A^n given by

$$M_A^n(x, Q^2) = \int \frac{dy_0^-}{2\pi} e^{ixp^+y_0^-} \langle P_A | \bar{\psi}_f(0) \frac{\gamma^+}{2} \psi_f(y_0^-) \prod_{i=1}^n \left[\int p^+ dy_i^- \theta(y_i^-) \hat{F}^2(y_i^-) \right] | P_A \rangle. \quad (26)$$

The integration $\int p^+ dy_i^-$ in Eq. (26) gives the nuclear size dependence [15]. And the operator $\hat{F}^2(y_i^-)$ is given by

$$\hat{F}^2(y_i^-) \equiv \int \frac{d\tilde{y}_i^-}{2\pi} \frac{F^{+\alpha}(y_i^-) F_\alpha^+(\tilde{y}_i^-)}{p^+} \theta(\tilde{y}_i^-). \quad (27)$$

Compare with the operator definition of gluon density, we can see that its expectation value can be related to the small- x limit of the gluon distribution, $\langle p | \hat{F}^2(y_i^-) | p \rangle \approx \lim_{x \rightarrow 0} \frac{1}{2} x G(x, Q^2)$, and is independent of y_i [10].

In order to evaluate the multi-field matrix element in Eq. (26), we approximate the expectation value of the product of operators to be a product of expectation values of the basic operator units in a nucleon state of momentum $p = P_A/A$:

$$\langle P_A | \hat{O}_0 \prod_{i=1}^n \hat{O}_i | P_A \rangle = A \langle p | \hat{O}_0 | p \rangle \prod_{i=1}^n \left[N_p \langle p | \hat{O}_i | p \rangle \right],$$

where N_p is the normalization. In a model of constant lab frame nucleus density $\rho(r) = 3/(4\pi r_0^3)$, we have

$$\int p^+ dy_i^- \theta(y_i^-) N_p \langle p | \hat{F}^2(y_i^-) | p \rangle = \frac{9}{16\pi r_0^2} (A^{1/3} - 1) \langle p | \hat{F}^2(y_i^-) | p \rangle \quad (28)$$

The factor $(A^{1/3} - 1)$ is taken such that the nuclear effect vanishes for $A = 1$. With the above model for $M_A^{(n)}$, we have

$$\frac{dW_{\mu\nu}^{(n)}}{dz_h} \approx \frac{1}{2} e_{\mu\nu}^T \sum_q e_q^2 A \phi_q(x_B, Q^2) \left[\frac{z_h \kappa^2 (A^{1/3} - 1)}{Q^2} \right]^n \frac{1}{n!} \frac{d^n}{dz_h^n} D_{q \rightarrow h}(z_h, Q^2) \quad (29)$$

The quantity κ^2 represent the characteristic scale of quark interaction with the medium [10]

$$\kappa^2 = \frac{3\pi\alpha_s(Q^2)}{4r_0^2} \langle p | \hat{F}^2(y_i) | p \rangle. \quad (30)$$

Summing the $A^{1/3}$ -enhanced contributions in Eq. (29) to all order in n , we have

$$\begin{aligned} \frac{dW_{\mu\nu}}{dz_h} &\approx \frac{1}{2} e_{\mu\nu}^T \sum_q e_q^2 A \phi_q(x, Q^2) \sum_{n=0}^N \frac{1}{n!} \left[\frac{z_h \kappa^2 (A^{1/3} - 1)}{Q^2} \right]^n \frac{d^n D_{q \rightarrow h}(z_h, Q^2)}{d^n z_h} \\ &\approx A \frac{1}{2} e_{\mu\nu}^T \sum_q e_q^2 \phi_q(x, Q^2) D_{q \rightarrow h} \left(z_h + \frac{z_h \kappa^2 (A^{1/3} - 1)}{Q^2}, Q^2 \right), \end{aligned} \quad (31)$$

where N is the upper limit on the number of quark-nucleon interactions. In deriving Eqs. (31) we have taken $N \approx \infty$ because the effective value of κ^2 is relatively small. Eq. (31) is the main result of this paper. It shows that the net effect of multiple scattering without induced radiation for a propagating quark in the medium is equivalent to a shift in the variable z for the quark fragmentation function $D_{q \rightarrow h}(z)$, which leads to a suppression of the hadron production rate. This is a result of the quantum interference of amplitudes of multiple scattering. Such a shift in z for the fragmentation function is very similar to the effect of the parton energy loss model proposed in Ref. [21]. The shift

$$\Delta z(z_h) = z_h \frac{\kappa^2 (A^{1/3} - 1)}{Q^2} \quad (32)$$

depends on only one parameter κ^2 and the medium length. The parameter $\kappa^2 \propto \lim_{x \rightarrow 0} x G(x, Q^2)$ with $G(x, Q^2)$ the gluon distribution function. It can be related to the λ^2 in LQS model for twist-4 quark-gluon correlation function $T_{qg}(x) = A^{4/3} \lambda^2 \phi_q(x)$ [17] by $\kappa^2 = (4\pi^2 \alpha_s / 3) \lambda^2$. The λ^2 has been estimated using Drell-Yan transverse momentum broadening and DIS momentum imbalance [17, 20], and was in the range of 0.01 – 0.1 GeV².

Using our result given in Eq. (31), we obtain the hadron production rate defined in Eq. (2) for SIDIS on a nucleus target A :

$$R^A \approx \frac{\sum_q e_q^2 \phi_q^A(x_B, Q^2) D_{q \rightarrow h}(z_h + \Delta z(z_h))}{\sum_q e_q^2 \phi_q^A(x_B, Q^2)}, \quad (33)$$

with $\Delta z(z_h)$ given in Eq. (32).

IV. THE QUARK MASS EFFECT

In the above derivation, we concentrated on the multiple scattering of light quarks and ignored the quark mass. If the stuck quark is a heavy quark, we then can not ignore the

quark mass. In this case, the initial quark momentum can not be approximated as xp . Instead, we have the quark momentum

$$k^\mu = xp^+ \bar{n}^\mu + \frac{m^2}{2xp^+} n^\mu, \quad (34)$$

with m the quark mass. Due to the on-shell condition $(k+q)^2 = m^2$, the final state δ -function is modified as

$$\delta((k+q)^2 - m^2) = \frac{1}{\sqrt{1 + 4m^2/Q^2}} \frac{x_{Bm}}{Q^2} \delta(x - x_B) \quad (35)$$

with

$$x_{Bm} = x_B \frac{1 + \sqrt{1 + 4m^2/Q^2}}{2}. \quad (36)$$

In addition, for additional scattering with each gluon pair in the medium, the interaction will contribute a factor

$$x_{Bm} \left[\frac{2}{1 + \sqrt{1 + 4m^2/Q^2}} \right]^2 \frac{2\pi\alpha_s}{3Q^2} \times \int \frac{dy_i^-}{2\pi} \frac{d\tilde{y}_i^-}{2\pi} \frac{e^{i(x_i - \tilde{x}_i)p^+ y_i^-}}{x_i - \tilde{x}_i - i\epsilon} \frac{e^{i(\tilde{x}_i - x_{i-1})p^+ \tilde{y}_i^-}}{\tilde{x}_i - x_{i-1} - i\epsilon} F^{+\alpha}(y_i^-) F_\alpha^+(\tilde{y}_i^-) \begin{cases} \frac{-1}{x_{i-1} - x_{Bm} + i\epsilon} & \text{(L)} \\ \frac{-1}{x_i - x_{Bm} - i\epsilon} & \text{(R)} \end{cases}. \quad (37)$$

Correspondingly, due to the multiple scattering with the medium, the shift $\Delta z(z_h)$ in fragmentation function for a heavy quark with mass m is

$$\Delta z_m(z_h) = z_h \left[\frac{2}{1 + \sqrt{1 + 4m^2/Q^2}} \right]^2 \frac{\kappa^2(A^{1/3} - 1)}{Q^2}. \quad (38)$$

From Eq. (38), we see that the z -shift for a heavy quark has a similar functional form to that of a light quark, except that it has an extra factor that depends on the quark mass. This mass dependent factor makes the z -shift smaller for a heavier quark. However, as we can see from Fig.6 and Fig.7, the fragmentation function of a heavy quark have very different z -dependence from that of a light quark. The z -shift in fragmentation function can result in very different hadron production ratio, even though they have similar forms of z -shift. Therefore, we expect that the net effect of multiple scattering for heavy meson production to be very different from that for light mesons.

V. NUMERICAL ESTIMATES AND COMPARISON WITH DATA

In order to compare with data [22], we compute the ratio of R^A for a nuclear target A to that of a deuterium target D :

$$R_M = \frac{R^A}{R^D} \approx \frac{\sum_q e_q^2 \phi_q^A(x_B, Q^2) D_{q \rightarrow h}(z_h + \Delta z(z_h))}{\sum_q e_q^2 \phi_q^D(x_B, Q^2) D_{q \rightarrow h}(z)} \frac{\sum_q e_q^2 \phi_q^D(x_B, Q^2)}{\sum_q e_q^2 \phi_q^A(x_B, Q^2)}. \quad (39)$$

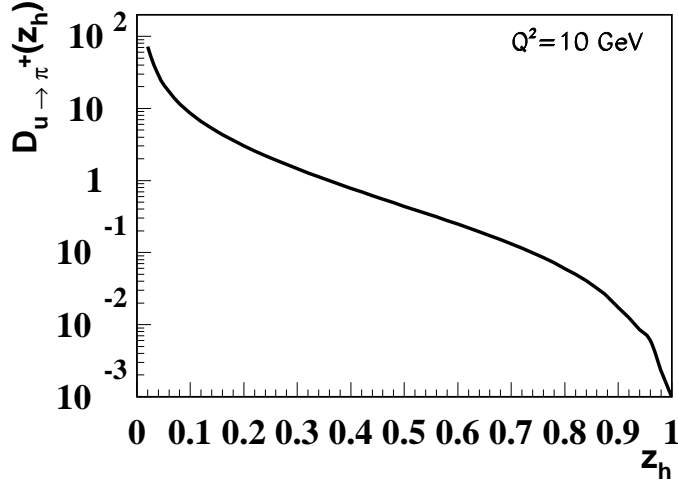


FIG. 6: u -quark fragmentation function given by Ref. [25].

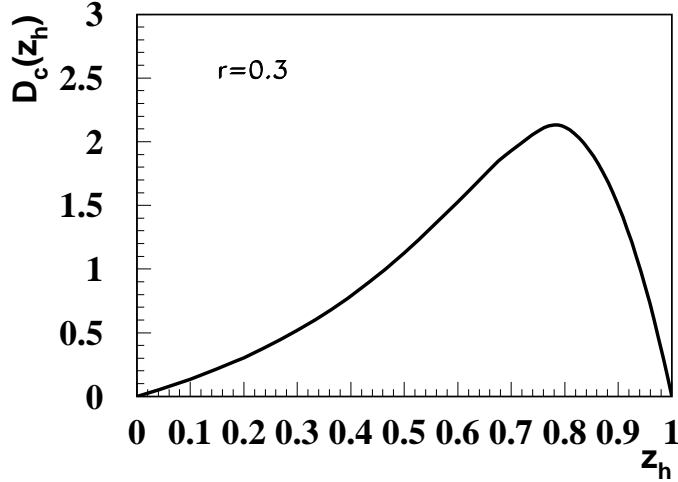


FIG. 7: Charm quark fragmentation function at $Q^2 = 9 \text{ GeV}^2$ from Ref. [28]. r is a parameter that represents the ratio of the constituent mass of the light quark to the meson mass.

The super script “A” and “D” represent the nuclear target of atomic weight A and the deuterium target, respectively.

To obtain the numerical estimate of the double ratio R_M in Eq. (39), we use the lowest order CTEQ6 parton distributions [23]. For the nuclear dependence of parton distribution, we use the parameterizations given in Ref. [24]. Figs. 8-11 compares our result with the data from HERMES experiment[22]. The experiment data points have x_B in the range of $0.084 - 0.1$, and the $Q^2 \sim 2.2 - 2.6 \text{ GeV}^2$. In plotting Figs. 8-11, we used the fragmentation function provided by Ref. [25]. The dot lines represent the result with double scattering only. The dashed curves represent the result when we sum to all order. We can see that our curve is slightly above the data, because our calculation only include multiple scattering without induced radiation. The induced radiation will give further suppression [7, 8] and

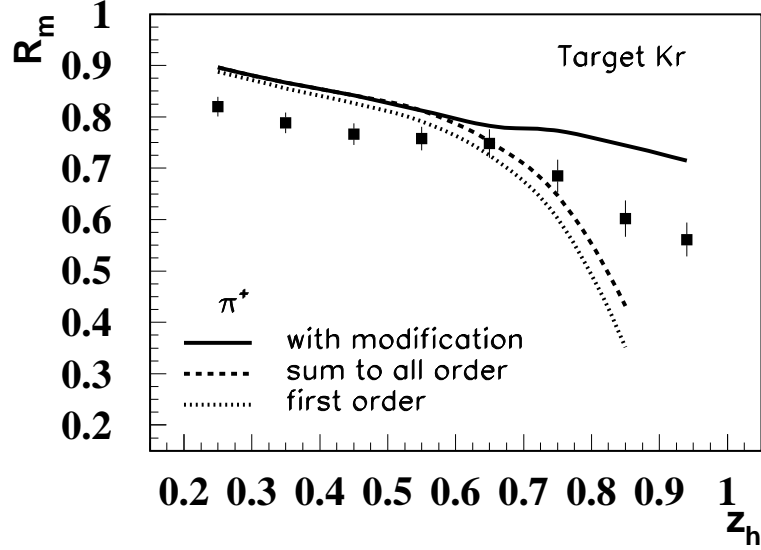


FIG. 8: The double ratio R_M of Eq. (39) for π^+ production with Krypton target, compared with HERMES data.

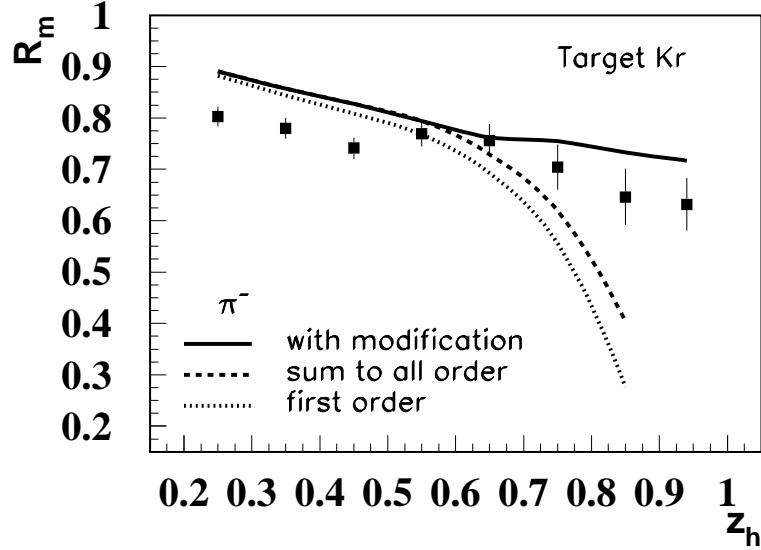


FIG. 9: The double ratio R_M of Eq. (39) for π^- production with Krypton target, compared with HERMES data.

brings down the curve. We also notice that at large z_h region, our curve is steeper than the data point. This is because our result sums the additional scattering to all order and it is not applicable for large z_h . At large z_h , the hadron forms early, and have shorter formation time. In this case, Summing the additional scatterings to all order is an unrealistic approximation. In order to take into account of the hadron formation time, which is proportional to $(1 - z_h)$

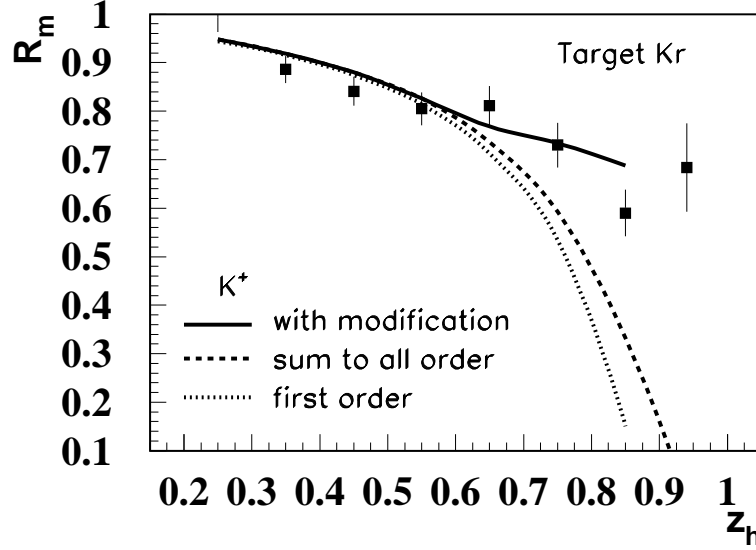


FIG. 10: The double ratio R_M of Eq. (39) for K^+ production with Krypton target, compared with HERMES data.

[26], we modify the z_h shift to be at large z_h

$$\Delta z(z_h) = z_h \frac{\kappa^2(A^{1/3} - 1)}{Q^2} \frac{(1 - z_h)}{1 - z_c} \quad \text{when} \quad z > z_c. \quad (40)$$

In Eq. (40), z_c is a parameter. In this model, we assume that when $z_h < z_c$, the hadrons will form outside of the nucleus, and we do not need to worry about the hadron formation time. We can apply our resummed result of Eq. (32) when $z_h < z_c$. When $z_h > z_c$, the hadron formation process may start early, and we use the modified $\Delta z(z_h)$ given in Eq. (40) to take into account of the formation time. The solid lines in Figs. 8-11 show our estimates when we use the above modified Δz , and choose $z_c = 0.6$. The curve is above the data points at large z_h , because here we did not consider the nuclear absorption of the pre-hadron state. The nuclear absorption of pre-hadron state should give additional suppression and bring down the curve a little more [26].

In Fig. 12, we plot the figure for D meson production in eA scattering. Due to the limit in collision energy, there is no data for D meson production from Hermes experiment. However, future Electron-ion Collider (EIC) experiments at Brookhaven should be able to observe the semi-inclusive D meson production [27]. In obtaining Fig. 12, we used the c -quark fragmentation function of Ref. [28]. From Eq.(39), we see that the ratio R_M is mainly determined by the shift $\Delta z(z_h)$ and the shape of fragmentation functions. Since the fragmentation function for light- and heavy-meson have very different z -dependence, as shown in Fig.6 and Fig.7, the shift in z_h results in very different double ratio R_M . At smaller z_h region, z_h may actually result in $R_M > 1$ for D mesons, due to the characteristic shape of the c -quark fragmentation function, as we can see from Fig. 7.

In Fig. 8-12, we only illustrate the size of the suppression due to the shift of z_h , which is caused by coherent multiple scattering without induced radiation. A more complete analysis should include other effects, such as induced radiation.

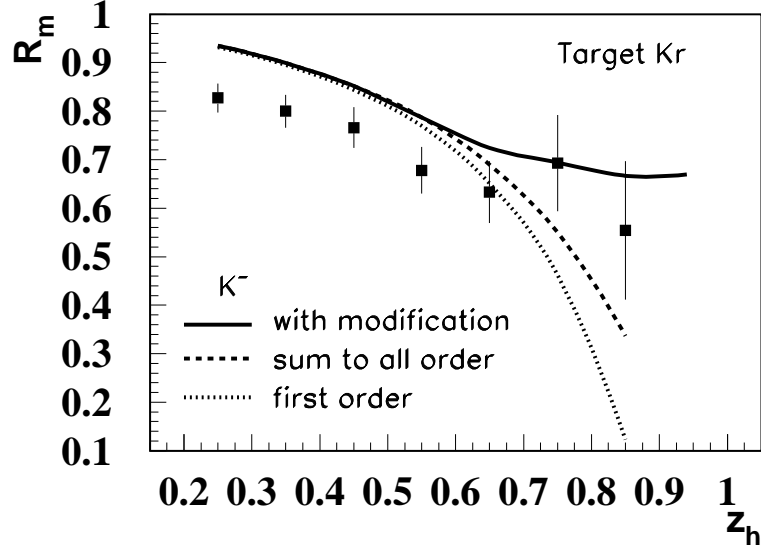


FIG. 11: The double ratio R_M of Eq. (39) for K^- production with Krypton target, compared with HERMES data.

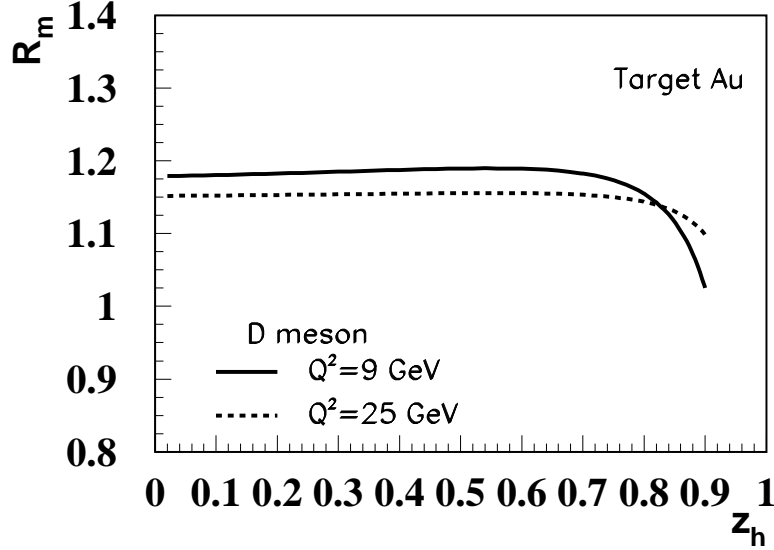


FIG. 12: Our estimate of double ratio R_M for D meson production with gold target at $Q^2 = 9 \text{ GeV}^2$ and $Q^2 = 25 \text{ GeV}^2$.

VI. SUMMARY AND OUTLOOK

In summary, we demonstrated that the coherent multiple scattering of a propagating quark with the medium, without the induced radiation, can also change the quark fragmentation or hadron's production rate. The net effect of leading power contributions in medium length is equivalent to a shift in the fragmentation function's $z_h \rightarrow z_h + \Delta z$. At

the lowest order, the shift Δz is given by an universal matrix element, which is proportional to $\lim_{x \rightarrow 0} xG(x, Q^2)$. We also show that for a quark with mass m , the shift will be smaller. Our result could be interpreted as the collisional energy loss, which is complementary to the energy loss of induced radiation. However, beyond the leading order, the separation of the collisional energy loss and that of induced radiation will depend on the factorization scheme and will not be unique, and need further study.

In this paper, we derived the effect of the radiationless multiple scattering in semi-inclusive DIS, our approach can be systematically generalized to hadron production in $p + A$ and $A + A$ collisions. Because of the convolution of two parton distributions, which are steep falling functions of parton momentum fraction x , the hadron production in hadronic collisions is dominated by the large z part of fragmentation functions, in particular, for heavy meson production [29]. As shown in Fig. 7, the heavy quark fragmentation functions are steep falling functions of z in large z region. As a result, depending on the momentum of the observed heavy meson, or the effective range of z , we expect that the radiationless multiple scattering will lead to a suppression of heavy meson production, similar to that in light hadron production.

Acknowledgments

This work was support in part by the U.S. National Science Foundation under Grant PHY-0340729.

-
- [1] S. S. Adler *et al.* [PHENIX Collaboration], Phys. Rev. Lett. **91**, 072301 (2003); and references therein.
 - [2] M. Gyulassy and X. n. Wang, Nucl. Phys. B **420**, 583 (1994). X. N. Wang, M. Gyulassy and M. Plumer, Phys. Rev. D **51**, 3436 (1995). R. Baier, Y. L. Dokshitzer, A. H. Mueller, S. Peigne and D. Schiff, Nucl. Phys. B **484**, 265 (1997). B. G. Zakharov, JETP Lett. **63**, 952 (1996); JETP Lett. **65**, 615 (1997). M. Gyulassy, P. Levai and I. Vitev, Nucl. Phys. B **594**, 371 (2001); Phys. Rev. Lett. **85**, 5535 (2000). U. A. Wiedemann, Nucl. Phys. B **588**, 303 (2000).
 - [3] S. S. Adler *et al.* [PHENIX Collaboration], Phys. Rev. Lett. **96**, 032301 (2006); J. Bielcik [STAR Collaboration], Nucl. Phys. A **774**, 697 (2006).
 - [4] Y. L. Dokshitzer and D. E. Kharzeev, Phys. Lett. B **519**, 199 (2001).
 - [5] M. H. Thomas, Phys. Lett. B **273**, 128 (1991). E. Braaten and M. H. Thoma, Phys. Rev. D **44**, 2625 (1991). P. Romatschke and M. Strickland, Phys. Rev. D **71**, 125008 (2005).
 - [6] M. G. Mustafa, Phys. Rev. C **72**, 014905 (2005). M. Djordjevic, M. Gyulassy, R. Vogt and S. Wicks, Nucl. Phys. A **774**, 689 (2006).
 - [7] X. f. Guo and X. N. Wang, Phys. Rev. Lett. **85**, 3591 (2000). [arXiv:hep-ph/0005044].
 - [8] X. N. Wang and X. f. Guo, Nucl. Phys. A **696**, 788 (2001) [arXiv:hep-ph/0102230].
 - [9] E. Wang and X. N. Wang, Phys. Rev. Lett. **89**, 162301 (2002).
 - [10] J. w. Qiu and I. Vitev, Phys. Rev. Lett. **93**, 262301 (2004) [arXiv:hep-ph/0309094].
 - [11] R. Brock *et al.*, Rev. Mod. Phys. **67**, 157 (1995).
 - [12] J. w. Qiu, Phys. Rev. D **42**, 30 (1990).
 - [13] J. w. Qiu, G. Sterman, Int. J. Mod. Phys. E **12**, 149 (2003).
 - [14] For example, see F.E. Close, J.-W. Qiu and D.G. Roberts, Phys. Rev. D **40**, 2820 (1989).

- [15] J. w. Qiu, Nucl. Phys. A **715**, 309 (2003).
- [16] J.-W. Qiu and G. Sterman, Nucl. Phys. **B353**, 105 (1991); **B353**, 137 (1991).
- [17] M. Luo, J. w. Qiu and G. Sterman, Phys. Rev. D **49**, 4493 (1994).
- [18] A.H. Mueller and J. w. Qiu, Nucl. Phys. **B268**, 427 (1986).
- [19] X. f. Guo, J. w. Qiu, W. Zhu, Phys. Lett. B **523**, 88 (2001).
- [20] X. f. Guo, Phys. Rev. D **58**, 114033 (1998).
- [21] X. N. Wang and Z. Huang, Phys. Rev. C **55**, 3047 (1997); X. N. Wang, Z. Huang and I. Sarcevic, Phys. Rev. Lett. **77**, 231 (1996).
- [22] A. Airapetian *et al.* [HERMES Collaboration], Eur. Phys. J. C **20**, 479 (2001).
- [23] J. Pumplin, D. R. Stump, J. Huston, H. L. Lai, P. Nadolsky and W. K. Tung, JHEP **0207**, 012 (2002).
- [24] K.J. Eskola, V.J. Kolhinen, and C.A. Salgado Eur. Phys. J. **C9**, 61 (1999). K.J. Eskola, V.J. Kolhinen, and P.V. Ruuskanen, Nucl. Phys. **B535**, 351 (1998).
- [25] S. Kretzer, Phys. Rev. D **62**, 054001(2000).
- [26] A. Accardi, nucl-th/0604041.
- [27] A. Deshpande, R. Milner, R. Venugopalan and W. Vogelsang, Ann. Rev. Nucl. Part. Sci. **55**, 165 (2005).
- [28] E. Braaten, K. m. Cheung, S. Fleming and T. C. Yuan, Phys. Rev. D **51**, 4819 (1995).
- [29] E. L. Berger, J. w. Qiu and X. f. Zhang, Phys. Rev. D **65**, 034006 (2002) [arXiv:hep-ph/0107309].